ELSEVIER

Ceramics International 25 (1999) 261–265

CERAMICS INTERNATIONAL

Crystallization kinetics of $Ba_{0.8}Sr_{0.2}TiO_3$ sols and sol–gel synthesis of $Ba_{0.8}Sr_{0.2}TiO_3$ thin films

Dinghua Bao*, Zhihong Wang, Wei Ren, Liangying Zhang, Xi Yao

Electronic Materials Research Laboratory, Xi'an Jiaotong University, Xi'an, 710049, People's Republic of China

Received 1 November 1997; accepted 5 February 1998

Abstract

Chemically homogeneous $Ba_{0.8}Sr_{0.2}TiO_3$ (BST) sols were synthesized using barium acetate, strontium acetate, and titanium tetra-n-butoxide as starting materials. The crystallization behaviour of the BST sols and thin films was studied by differential thermal analysis (DTA) and X-ray diffraction (XRD). The kinetics of crystallization was studied by applying the DTA measurement carried out at different heating rates. The effective activation energy of crystallization associated with the formation of perovskite phase was measured as 270.8 kJ mol^{-1}. The Avrami exponent n (reaction order) is about 1, which suggests that the growth of perovskite phase is diffusion-controlled. The calculated half-life time indicates that the minimum temperature for the crystallization is 600°C. The BST thin films were prepared on Pt-coated silicon substrates from the sols. The films annealed at 650°C have good perovskite crystallinity without the existence of second phase.

Keywords: $Ba_{08}Sr_{0.2}TiO_3$; Crystallization kinetics; Sol–gel technique; Thin film

1. Introduction

Barium strontium titanate ($Ba_xSr_{1-x}TiO_3$,BST) is a dielectric material with excellent dielectric properties such as high dielectric constant, small dielectric loss, low leakage current, large dielectric breakdown strength. It is thought to be the most promising dielectric material for the memory cell capacitors in dynamic random access memory (DRAM) with very large scale integration (VLSI) [1,2]. Besides, the properties of $Ba_xSr_{1-x}TiO_3$ can be tailored for specific applications including piezoelectric transducers and optical signal processing, [3,4]. Recently, there have been some studies on the preparation of the BST thin films.

From a material view point, BST is the solid solution of $BaTiO_3$ and $SrTiO_3$. $BaTiO_3$ is a ferroelectric material with the Curie temperature T_c of 120°C, while $SrTiO_3$ is paraelectric material with no ferroelectric phase transition. Therefore, T_c of BST can be suitably controlled by adjusting the ratio of Ba to Sr. At room temperature, it is known that the solid solution system is in a ferroelectric phase when Ba content is in a range of 0.7–1.0, and in a paraelectric phase when Ba content is less than 0.7 . The composition of BST used in the present study can be represented by $Ba_{0.8}Sr_{0.2}TiO_3$, i.e. $x = 0.8$.

A variety of techniques have been used to prepare $(Ba,Sr)TiO_3$ thin films such as sputtering [5], pulsed laser deposition (PLD) [6], metalorganic chemical vapour deposition (MOCVD) [7], sol–gel [8], etc. Among these methods, sol–gel technique has obtained much interest because of its many advantages such as easier composition control, better homogeneity, lower processing temperature, lower cost, easier fabrication of large area films [9]. Recently, some highly oriented or epitaxial thin films were obtained using this technique [10,11]. However, there appears to be relatively few reports on the preparation of BST thin films by the sol-gel technique [12]. Further, very limited information has beenknown on the kinetics of pcrovskite phase formation [13].

The aim of this research is to study the crystallization behaviour of BST, to determine some important parameters in the kinetic equations that described the process of crystallization, and further, to prepare BST thin films for application of DRAM.

* Corresponding author. Fax: +86-29-3268794

0272-8842/99/$—see front matter
PII: S0272-8842(98)00034-0

2. Experimental procedure

BST precursor solutions were synthesized using strontium acetate semihydrate [$Sr(CH_3COO)_2 \cdot \frac{1}{2}H_2O$] and barium acetate [$Ba(CH_3COO)_2$], and titanium tetra-*n*-butoxide [$Ti(OC_4H_9)_4$] as source materials. Glacial acetic acid and 2-methoxyethanol were selected as solvents. Strontium acetate and barium acetate were initially dissolved in glacial acetic acid, titanium tetra-*n*-butoxide mixed with 2-methoxyethanol was added dropwise to the above solution with constant stirring, then the solution was filtered. The viscosity of the solution was controlled by varying the 2-methoxyethanol content. Addition of 2-methoxyethanol also improved the wetness and uniformity of the coating on the substrate [4]. The resulting concentration of the solutions was 0.2 mol l^{-1}. The precursor solutions were spin-coated on fused quartz substrates by a spinner operating at a speed of 3000 rpm for 30 s. After the coating process, the films were kept in air for 1 h to form gel films by the hydrolysis and polymerization. They were then slowly heated at a rate of 2°C min^{-1} to a prefiring temperature of 300°C for the decomposition of residual organics, and finally cooled to room temperature. The above process of coating and prefiring was repeated several times to increase the thickness of the films. The deposition conditions were the same for all samples.

As-prefired films were amorphous in nature. Annealing at higher temperatures was needed to convert the amorphous structure into a crystalline structure.

Differential thermal analysis (DTA) was performed by a Dupont TA-2000 thermal analysis system. The structure of the thin films was analysed by a Rigaku D/max-2400 X-ray diffractometer with CuK_α radiation.

3. Results and discussion

Fig. 1 shows DTA curve of the BST sol. The DTA curve indicates that the evaporation of residual water and acetic acid occurs at about 100°C and the evaporation of 2-methoxyethanol at 130°C. The pyrolysis of residual organics is basically characterized by the two-step exothermic process which occurs between 350 and 460°C. Analysis of XRD measurement suggests that the exothermic peak at 602°C was associated with the formation of perovskite phase. Further analysis using FTIR spectra shows that the formation of the perovskite BST was accompanied with the appearance of the peak related to the vibration of the TiO_6 octahedron unit at 550 cm^{-1}.

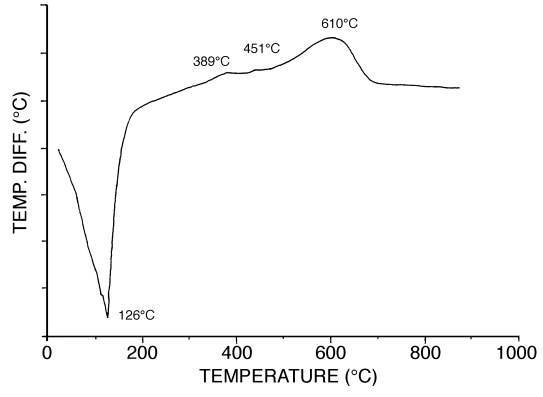

Fig. 1. DTA curve of the BST sol measured with a heating rate of 20°C min^{-1}.

The effective Arrhenius activation energy (E_a) for crystallization of perovskite phase was determined by Kissinger equation. The method is based on the dependence of the crystallization peak temperature (T_M) on the DTA heating rate (Q) as follows [15]:

$$\mathrm{Ln}C + \mathrm{Ln}\nu_0 - \frac{E_a}{RT_M} - \mathrm{Ln}E_a = \mathrm{Ln}\left(\frac{Q}{RT_M^2}\right) \quad (1)$$

with $C = n[-\mathrm{Ln}(1-x)]^{(n-1)/n}$

where T_M is the temperature for the maximum rate of phase conversion, i.e. the crystallization peak temperature. Q the constant heating rate in the DTA experiment, E_a the activation energy for crystallization (J mol^{-1}), R the gas constant (8.314 J mol^{-1}), T the absolute temperature. ν_0 is a pre-exponential factor for crystallization appearing in the Arrhenius expression of the effective reaction-rate constant, k, whose temperature dependence is generally expressed by the Arrhonius equation:

$$k = \nu_0 \exp\left(-\frac{E_a}{RT}\right) \quad (2)$$

or taking natural logarithms,

$$\mathrm{Ln}k = \mathrm{Ln}\nu_0 - \frac{E_a}{RT} \quad (3)$$

According to the transition-state theory, ν_0 can be identified with the vibration (parallel to the reaction coordinate) frequency of the atom in the transition state incorporating into a new growing phase (nucleus) and is, therefore, a frequency factor (s^{-1}).

The fraction of the transformed phase (x) at time t is expressed by k according to the following well-known phenomenological Johnson–Mehl–Avrami (JMA) equation [16],

$$x = 1 - \exp[-(kt)^n] \quad (4)$$

Taking natural logarithms and rearranging Eq. (4), we have

$$\mathrm{Ln}[-\mathrm{Ln}(1-x)] = n\mathrm{Ln}k + n\mathrm{Ln}t \quad (5)$$

where x is the volume fraction crystallized after time t, n the Avrami exponent, a dimensionless parameter, n value depends on the mechanism of nucleation/growth of a new phase. The relationship between them is shown in Table 1 [17,18].

Four different heating rates (5, 12, 20, and 30°C min^{-1}) were employed to estimate E_a for the formation of the perovskite BST. The peak temperature (T_M) dependence of heating rate is listed in Table 2 . It can be seen from Table 2 that the results are in accordance with published literature data, that is, the crystallization peak temperature increases with heating rate. The effective activation energy can be obtained from the slope of a plot of $-\mathrm{Ln}(\frac{Q}{RT_M^2})$ versus $1/T_M$ [Eq. (1)] and is approximately 270.8 kJ mol^{-1}.

The Avrami exponent or the reaction order (n) can also be estimated from the DTA curves recorded at different heating rates. In a given DTA curve, the reaction order (n) can be calculated from the following relation [19]:

$$n = 1.26I^{1/2} \quad (6)$$

where I is the peak shape factor. At the heating rate of 20°C min^{-1}, I is 0.4827, therefore, n is 0.875. The result suggests that the growth of perovskite phase is a diffusion-controlled process [13].

Considering the case of $n=1$, the half-life time ($t_{1/2}$) can be directly calculated by substituting $x=1/2$ into Eq. (4), namely,

$$t_{1/2} = (\mathrm{Ln}2)/k \quad (7)$$

To obtain k at various temperatures we must firstly know the frequency factor ν_0 in Eq. (2). For $n=1$, the constant C in Eq. (1) is 1. In this case, the frequency factor ν_0, can be directly obtained from Eq. (1).

$$\nu_0 = (^{QE_a}/_{RT_M^2}) \cdot \exp(^{E_a}/_{RT_M}) \quad (8)$$

By Eq. (8), ν_0 was calculated to be 8.694×10^{15} min^{-1}.

The effective reaction-rate constant (k) and the half-life time ($t_{1/2}$) for various transformation temperatures can be calculated from Eqs. (2) and (7), respectively. The calculated results are shown in Figs. 2 and 3, respectively. As shown in Fig. 2, the value k decreases with increasing temperature. At 500°C, k is

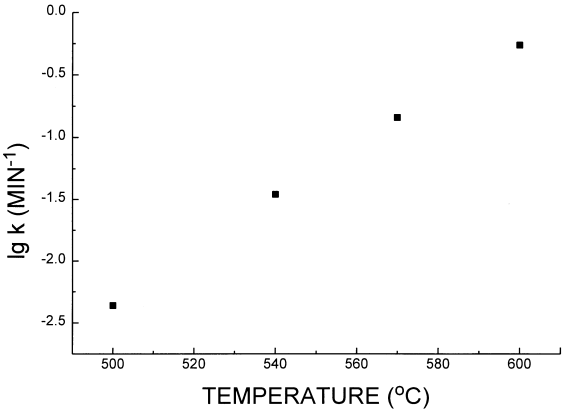

Fig. 2. Dependence of effective reaction-rate constant on transformation temperature.

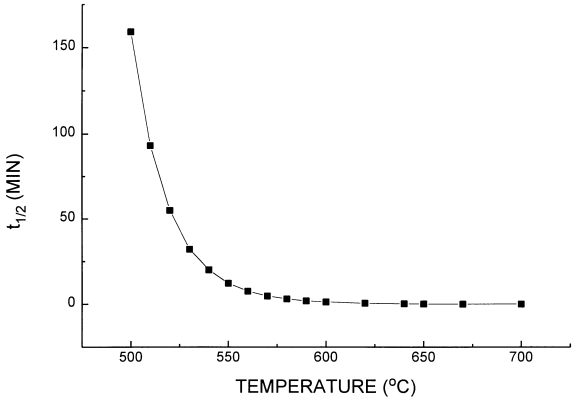

Fig. 3. Half-life time of BST sol as a function of temperature.

Table 1
Values of Avrami exponent n for various crystallization mechanisms

Mechanism	Avrami exponent n
Three-dimensional growth	4
Two-dimensional growth	3
One-dimensional growth	2
Surface nucleation	1

Table 2
Crystallization temperature of BST sol as a function of the heating rate

Heating rate, Q (K min^{-1})	Peak temperature, T_M (K)
5	851.43
12	872.84
20	883.14
30	891.2

Table 3
Data of crystallization kinetics of sol–gel-derived $PbTiO_3$, PZT, and BST powders

Material	Form	ν_0 (min^{-1})	E_a (kJ mol^{-1})	K (min^{-1}) at 500°C
$PbTiO_3$	Powder	1.0×10^{17}	265	1.2×10^{-1}
PZT	Powder	6×10^{19}	255	3.5×10^{2}
BST[13]	Powder	8.8×10^{23}	404	4.4×10^{-4}
BST (this study)	Powder	8.694×10^{15}	270.8	4.36×10^{-3}

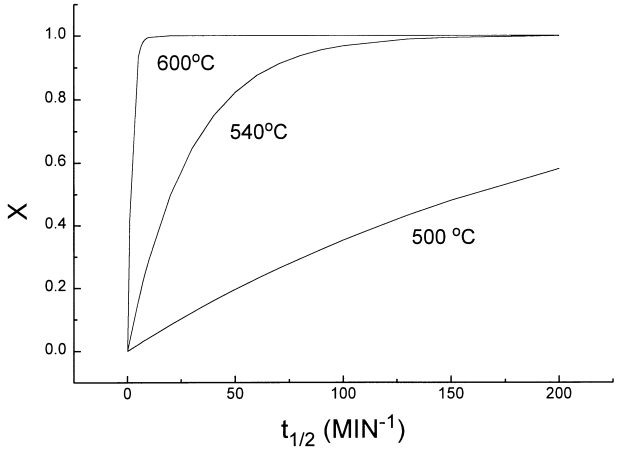

Fig. 4. Calculated isothermal transformation kinetics for the conversion to perovskite phase.

$4.36\times10^{-3}\,min^{-1}$. For comparison, data of crystallization kinetics of sol-gel-derived $PbTiO_3$, PZT, BST powders are summarized and listed in Table 3 [13]. It can be found that the activation energies for $PbTiO_3$ powder and PZT powder are 265 and 255 kJ mol^{-1}, respectively, which are close to that of BST sol in our study (270.8 kJ mol^{-1}). However, the reaction-rate constant of $PbTiO_3$ ($0.12\,min^{-1}$) is much larger than that of BST ($4.36\times10^{-3}\,Min^{-1}$) in our study, which indicates that the rate of perovskite formation from the $PbTiO_3$ gel is approximately 28 times faster than that for the BST sol. The rate of perovskitc phase formation in the PZT system seems to be even faster, i.e. about 8000 times. But, it is notable that the rate of perovskite phase formation in our study is about 10 times faster than that for the BST xerogel reported by Ref. 13. It can be seen from Fig. 3 that the time needed for the conversion to

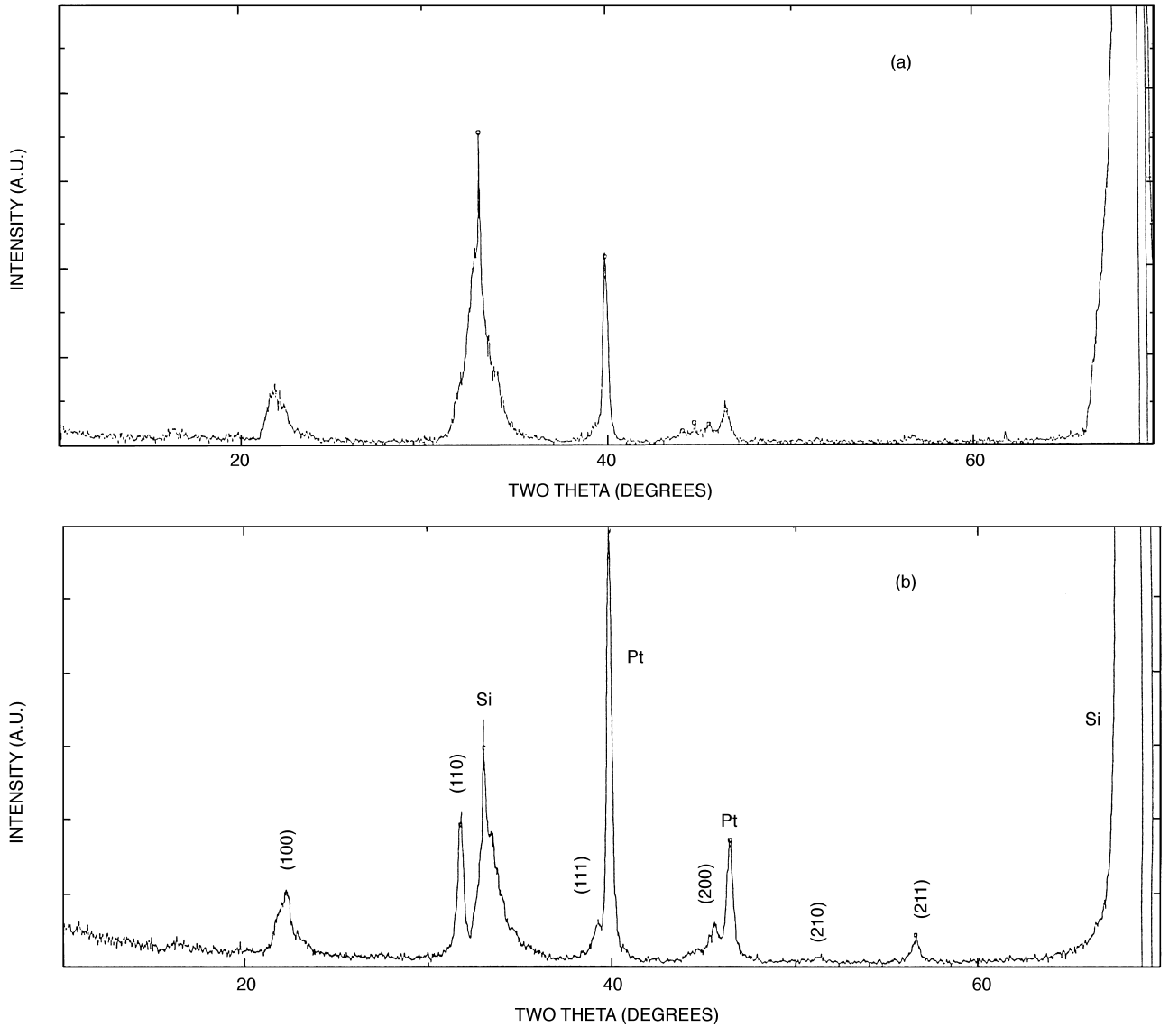

Fig. 5. The XRD patterns of the BST thin films annealed at (a) 550°C, and (b) 650°C, respectively, for 2 h.

the perovskite phase increases sharply (almost exponentially) with decreasing temperature when heat treated temperatures are below 550°C, and this suggests that the minimum temperature for the crystallization is approximately 600°C. This result is consistent with the XRD experiment. Hwang et al. also reported that the deposition of B ST thin films with good quality required high processing temperature (600°C or above), because of the difficulty in the formation of perovskite phase [20].

Fig. 4 shows the calculated isothermal transformation kinetics for the conversion to perovskite phase in the BST sol. The transformed fraction x was calculated from Eq. (4) with $n=1$ and the reaction-rate constants k at various transformation temperatures were estimated using the values of E_a and v, estimated previously (i.e. $270.8\,\mathrm{kJ\,mol^{-1}}$ and $8.694\times10^{15}\,\mathrm{min^{-1}}$, respectively). As shown in Fig. 4, the rate of perovskite formation increases rapidly with temperature.

BST thin films were prepared from the BST precursor solutions. The XRD patterns of the BST thin films are given in Fig. 5. It can be seen that the formation of perovskite phase completes at 650°C. This is consistent with the above result of crystallization kinetics.

4. Conclusion

BST sols were synthesized using barium acetate, strontium acetate, and titanium tetra-*n*-butoxide as starting materials. Johnson–Mehl–Avrami, and Kissinger equations were used to study crystallization kinetics of perovskite formation. The Avrami exponent n was found to be close to 1, which indicates that the perovskite nucleation/growth is a diffusion-controlled process. The effective activation energy of perovskite crystallization calculated is $270.8\,\mathrm{kJ\,mol^{-1}}$. BST thin films were prepared by a sol-gel technique. The thin films annealed at 650°C have good perovskite crystallinity without the existence of second phase.

Acknowledgement

The authors thank the National Natural Science Foundation of China for financial support.

References

[1] H.F. Cheng, J. Appl. Phys. 79 (1996) 7965.
[2] D.M. Tahan, A. Safari, L.C. Klein, J. Am. Ceram. Soc. 79 (1996) 1593,
[3] A. Nazeri, M. Kahn, T. Kidd, J. Mater. Sci. Lett. 14 (1995) 1085.
[4] D. Roy, S.B. Krupanidhi, Appl. Phys. Lett. 62 (1993) 1056.
[5] K. Abe, S. Komatsu, J. Appl. Phys. 77 (1995) 6461.
[6] S.G. Yoon, J.C. Lee, A. Safari, J. Appl. Phys. 76 (1994) 2999.
[7] T. Kimura, H. Yamauchi, H. Machida, H. Kokubon, M. Yamada, Jpn J. Appl. Phys. 33 (1994) 5129.
[8] J. Kim, S.I. Kwun, J.G. Yoon, in: P.K. Pandey, M. Liu, A. Safari (Eds.), Proc. Tenth IEEE Inter, Symp. Appl. Ferro., (PA, USA, 1994), p. 423.
[9] D.H. Bao, H.S. Gu, A.X. Kuang, Ferroelectrics, 188 (1996) 73.
[10] H.S. Gu, D.H. Bao, S.M. Wang, A.X. Kuang, Thin Solid Films, 283 (1996) 81.
[11] D.H. Bao, A.X. Kuang, H.S. Gu, Phys. Stat. Sol. (a) 163 (1997) 67.
[12] D. Tahan, A. Safari, L.C. Klein, in: P.K. Pandey, M. Liu, A. Safari (Eds.), Proc. Tenth IEEE Inter. Symp. Appl. Ferro., (PA, USA, 1994), p. 427.
[13] S.I. Jang, B.C. Choi, H.M. Jang, J. Mater. Res. 12 (1997) 1327.
[14] P.C. Joshi, S.B. Krupanidhi, J. Appl. Phys. 73 (1993) 7627.
[15] H.E. Kissinger, Anal. Chem. 29 (1957) 1702.
[16] V. Znidarsic, P.O. Kolar, J. Mater. Sci. 26 (1991) 2490.
[17] P. Balaya, C.S. Sunandana, J. Non-Cryst. Sol. 162 (1993) 253.
[18] S. Yilmaz, O.T. Ozkan, V. Gunay, Ceram. Inter. 22 (1996) 477.
[19] Z.Q. Cai, Thermal Analysis, Higher Education Press, Beijing, 1993, p. 115.
[20] C.S. Hwang, S.O. Park, H.J. Cho, C.S. Kang, S.I. Lee, M.Y. Lee, Appl. Phys. Lett. 67 (1995) 2819.